Phtalocyanine and *meso*-tetraphenylporphine effects on TiO_2/CdS nanocomposites photoactivity

M.C. ROSU*, R.C. SUCIU, M. D. LAZAR, I. BRATU
National Institute for Research and Development of Isotopic and Molecular Technologies, 65-103 Donath Street, 400293, Cluj-Napoca, Romania

TiO_2 is extensively studied for photoelectrochemical applications due to its interesting chemical, electrical and optical properties. However, TiO_2 has some limitations due to high band gap and, as consequence, an absorption in the ultraviolet region of solar spectrum. The effects of phtalocyanine and *meso*-tetraphenylporphine, as sensitizer dyes, on TiO_2/CdS nanocomposites were investigated in order to extend the absorption spectra of TiO_2 in the visible area and to improve its photocatalytic efficiency. The structural/morphological properties of the TiO_2/CdS-sensitized nanocomposites have been studied by X-ray diffraction, FTIR spectroscopy and microscopy and the optoelectronic properties have been investigated using UV-VIS absorption spectroscopy and spectrofluorimetry.

(Received June 2, 2011, accepted November 23, 2011)

Keywords: Nanocomposites, TiO_2, CdS, Phtalocyanine, meso-Tetraphenylporphine

1. Introduction

Titanium dioxide is one of the most interesting semiconductor oxides, which opened an important chapter in the photoelectrochemistry field. It shows non-toxicity and biocompatibility, chemical stability, corrosion resistance, photocatalytic potential and optoelectronic properties and it is found in considerable quantities at an affordable price [1-4]. TiO_2 is an n-type semiconductor due to oxygen vacancies [5-9] and it has a large band gap (3.0-3.2 eV) [10 – 11]. As a consequence, it absorbs UV radiation at wavelength $\lambda < 390$ nm and therefore, TiO_2 exhibits photoactivity in a narrow region of the incident solar light reaching the surface of the earth (~5%) [11-13 12 - 14]. In this way, different methods are used to modify TiO_2 nanoparticles [14 15], such as doping, sensitizing with inorganic/organic compounds or associating with other semiconductors [11, 16, 17].

Cadmium sulphide (CdS) is an n-type semiconductor with a band gap of 2.42 eV; it absorbs the electromagnetic radiation at ~ 495 nm, namely in visible range, the largest region of the solar spectrum (ca. 46%) [13, 18-20]. Therefore, it is a promising material with suitable properties (easy fabrication and long lifetimes) and higher photoactivity (relatively narrow band gap, optical absorption) [20, 21] for the use in solar cells, thin film transistors, display devices, semiconductor lasers and X-ray detectors [18, 28]. The association of TiO_2 with CdS can induce synergistic effects, such as an efficient charge separation, a recombination probability of the electron–hole pairs diminished and an enhancement of photostability [13, 19, 23, 243] with positive effects on photoelectrochemical properties and photocatalytic activity [19, 20, 25].

The sensitizing of semiconductors with phtalocyanine and porphyrin-based compounds is considered other way to obtain more efficient photoelectrodes. Porphyrin-based dyes are suitable as photosensitizers in solar cells due to their capability of photon absorption in the light visible domain, namely in the region of 400–450 nm (B or Soret band) as well as 500–700 nm (Q bands). This behavior leads to enhancing the efficiency in visible light absorption of the semiconductor materials and increasing its photocatalytic activity [26-28]. Phtalocyanines have structures very similar to porphyrins, in exchange they have superior chemical/photochemical properties and thermal stability due to their rigid structures. Also, they show absorption in the UV (Soret band) and the near IR (Q band) spectral regions [29-33]. The mechanism of sensitizing involves adsorption of dye molecules on the semiconductor surface by physical or chemical interactions, and electron injection from the excited dye molecule into the conduction band of the semiconductor, under visible light, causing an enhancing photoactivity of semiconductor [34, 35].

The improvement of TiO_2/CdS nanocomposite photoelectrocatalytic performance by sensitizing them with phtalocyanine and *meso*-tetraphenylporphine dyes was the objective of this study.

2. Experimental details

2.1. Materials

TiO_2 powder P25 (anatase:rutile ratio = 4:1) was kindly provided from *Degussa* AG, Germany; CdS was obtain from *Aldrich*, Germany. The conductive indium tin oxide glass (ITO, sheet resistance ≤ 20 Ω/square) were procured from *Praezision Glas&Optik*, Germany. The additives used to obtain the paste of TiO_2/CdS were: agar bacteriological (*Oxoid Limited*, England), acetylacetone

(*Merck*, Germany) and Tween 80 (*Merck*, Germany). The dyes used for sensitized TiO_2/CdS nanocomposites were phtalocyanine (*Fluka*, USA) and *meso*-tetraphenylporphine low chlorine (*Alfa Aesar*, Germany). The dichloromethane (*Fluka*, Germany) as solvent was added to prepare the dye solutions.

2.2. Preparation of TiO_2/CdS nanocomposites

In order to obtain a composite paste, TiO_2 and CdS powders (4:1 mass ratio) were placed in a mixture of agar bacteriological solution 0.01% and acetylacetone:Tween 80 in proportion of 2:1 volumetric ratio in order to obtain a better dispersion and particle uniformity and to facilitate also the spreading onto the conductive glass substrate. The homogenized paste (by magnetic stirring) was deposited onto ITO glass by spin-coating (5", 1000 rpm) and then, the samples were dry freezed in the lyophilizer (*Christ Alpha 1-4 LD*, Germany) at -60.7 °C and 0.028 mbar. In the next step, the dried samples were annealed at 450 °C for 30 min with 5 °C/min temperature increasing ramp (a treatment usually used to remove the organic additives) to establish the electrical contact between TiO_2/CdS and conductive ITO glass, to improve the composites crystallinity, to induce higher degree of porosity and greater thickness.

2.3. The sensitizing of the TiO_2/CdS composites

The dyes used for sensitized TiO_2/CdS nanocomposites were: phtalocyanine (Pc) and *meso*-tetraphenyl-porphine (TPP) (Fig. 1).

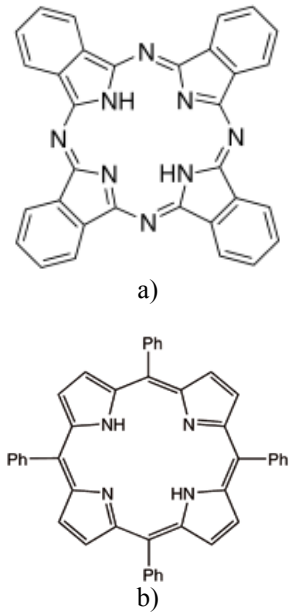

Fig. 1 Chemical formula of: a) phthalocyanine; b) meso-tetraphenylporphine.

It was prepared three different solutions (in dichloromethane as solvent) having the same concentration ($2x10^{-4}$M): Pc, TPP and Pc/TPP solutions. Pc/TPP solution was obtained by mixing in 1:1 volumetric ratio of two initial solutions. Still warm at 100°C, the TiO_2-based composites on ITO glass were immersed in prepared solutions and three samples were obtained: TC_{Pc}, TC_{TPP} and $TC_{Pc/TPP}$, depending on the dye solution used. Another sample, named TC, was intentionally left non-sensitized, as the standard-sample.

2.4. Characterization of TiO_2/CdS nanocomposites and solutions of Pc and TPP

X-ray diffraction (XRD) measurements were performed using a BRUKER D8 Advance X-ray diffractometer with nickel-filtered CuKα radiation (40 kV and 40mA). The UV–VIS spectra were obtained using a JASCO V-550 spectrometer. The fluorescence measurements were carried out with ABL&E JASCO V 6500 spectrofluorimeter. The FT/IR spectra were recorded on a JASCO FT/IR-6100 Fourier Transform Infrared Spectrometer using KBr pellet technique. The surface morphology of TiO_2/CdS samples was obtained by FT/IR microscopy (JASCO IRT – 3000 Irtron Infrared Microscope). The N_2 adsorption–desorption isotherms were measured with a Sorptomatic 1990 apparatus (Thermo Electron Corporation) used for specific surface area, pore volume and pore radius determinations.

3. Results and discussion

3.1. X-Ray diffraction studies

Fig. 2 shows the XRD patterns of all TiO_2/CdS nanocomposites. The XRD peaks for all samples are found to indicate the presence of anatase phase (101), (004) and (200) crystal planes (PDF card n. 21-1272), rutile (110) crystal plane (PDF card n. 21-1276), and also the presence of CdS cubic phase (1 1 1) and (2 0 0) crystal planes (PDF card n. 89-0440) (Figure 2a). In the 5-25^o 2θ domain, probably due to their crystallization after solvent evaporation, the sensitized samples were found containing also the crystalline phase of dyes, namely phtalocyanine [36] and *meso*-tetraphenylporphine [37].

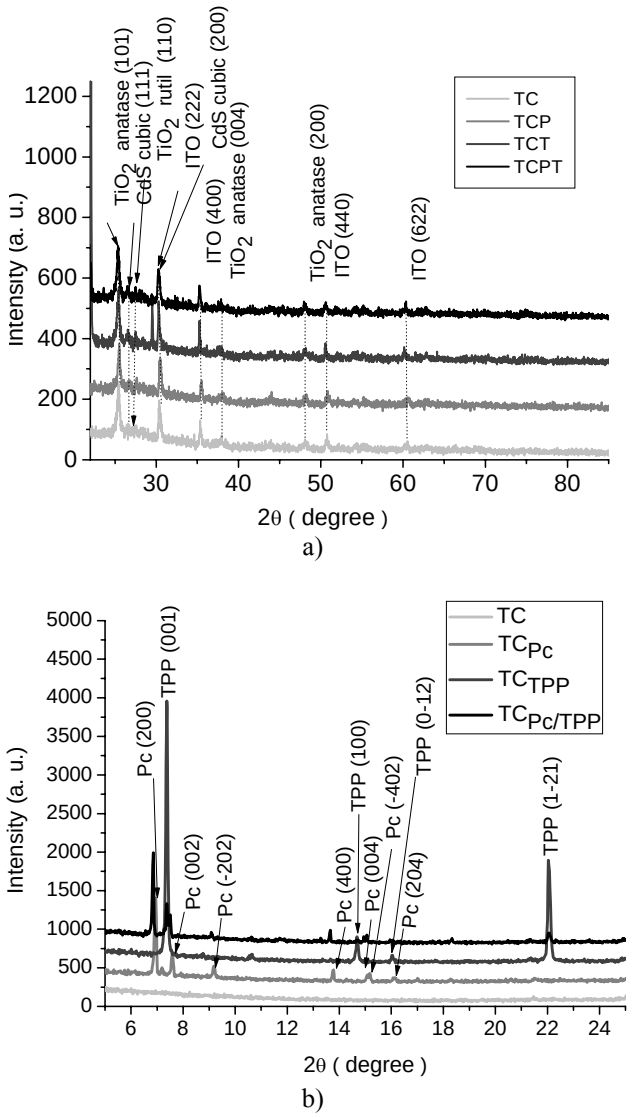

Fig. 2 X-ray diffraction patterns of TiO_2/CdS-based samples: a) 25-85° 2θ and b) 5-25° 2θ domain.

3.2. UV-VIS absorption characteristics

The normalized UV-VIS absorption spectra of Pc, TPP and Pc/TPP in dichloromethane are presented in Figure 3a. The absorption spectrum of the TPP shows two sets of bands due to the electronic transitions from the ground state (S_0) to the lowest singlet excited states S_1 (Q state) and S_2 (B state) [38]. The $S_0 \rightarrow S_1$ transition gives weaker absorptions associated with the higher wavelengths (500-700 nm/visible region), while $S_0 \rightarrow S_2$ transition produces the broad intense band in near UV region (400-450 nm), according to the Q bands and Soret band, respectively. The spectral absorptions appear due to the electronic transitions π – π* of the aromatic porphyrin orbitals [26,27,29,31,38]. The Soret bands broadening are due mainly to aggregation of porphyrins or a significant number of monomeric porphyrins at the surface area [29, 39]. The UV-VIS spectrum of Pc exhibits two bands with a lower intensity in the red visible region (Q bands) attributed to the π – π* transition in the Pc ring, in accordance with the transition from the highest occupied molecular orbital (HOMO) to the lowest unoccupied molecular orbital (LUMO). The band at 417 nm (Soret band), with a shoulder at 400 nm, is associated with the mixed π – π* transition and *n* – π* transitions [39]. In visible spectral range of Pc two absorption bands appear at 690 nm and 655 nm with a shoulder at 635 nm; these bands are attributed to monomeric phtalocyanine [41]. The absorption spectrum of Pc/TPP shows, by bands described, mainly the contribution of TPP, and also a weak absorption at 690 nm ascribed to Pc absorption in red visible region.

The TiO_2/CdS nanocomposites (Figure 3b) exhibit a strong absorption peak at 340 nm. There are no major changes in the absorption spectra, mainly due to physical adsorption of dyes on surface nanocomposite (by absence of anchoring groups dye structures). However, the appearance of weak absorption band at 420 nm for TC_{TPP} and $TC_{Pc/TPP}$ samples can be seen, due to strong absorption of TPP at this wavelength, which proves its presence on the surface of composites.

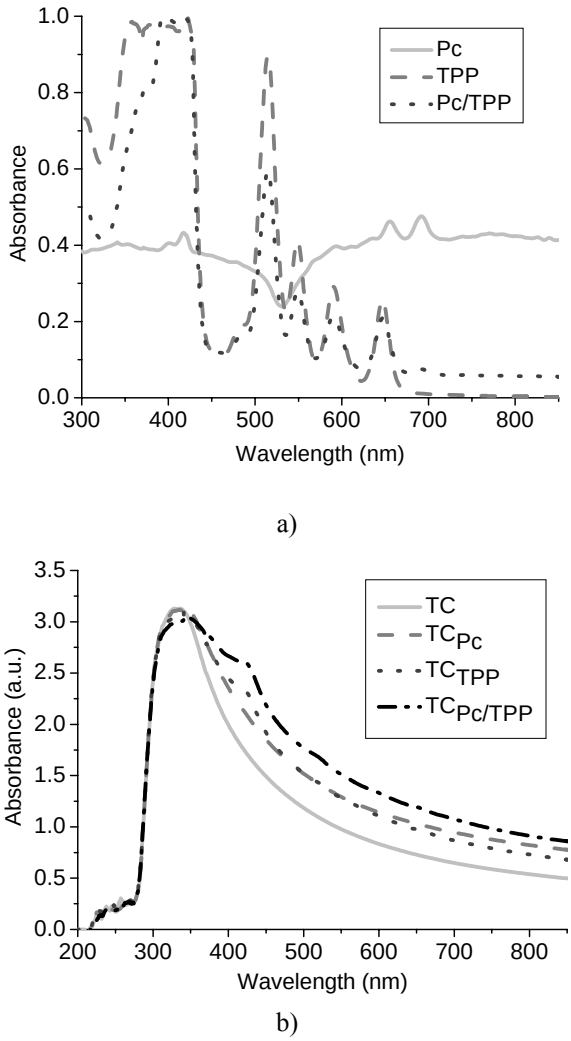

Fig. 3. a) Normalized UV-VIS spectra of PC, TPP and Pc/TPP in dicholorometane and b) typical UV-VIS spectra of TC, TC_{Pc}, TC_{TPP} and $TC_{Pc/TPP}$ samples.

3.3. Optical band gap determination

The band gap energies of all TiO_2/CdS samples were determined from UV-VIS spectra by linear extrapolation. The edges of the absorption of the TiO_2/CdS nanocomposites were shifted to visible region. Thus, the values of band gap energy in direct transition were higher than TiO_2 band gap energy (3.0-3.2 eV) and lower than a CdS (2.4 eV) one, also through the contribution of dye molecules adsorbed on the surface nanocomposites (Table 1).

Table 1. The values of band gap energy in direct transition for all samples.

Sample's name	Band gap energy value (eV)
TC	2.96
TC_{Pc}	2.82
TC_{TPP}	2.73
$TC_{Pc/TPP}$	2.54

3.4. Fluorescence characteristics

The photoluminiscence behavior of Pc, TPP and Pc/TPP have been investigated in dichloromethane and the fluorescence emission spectrum (λex = 600 nm) is shown in Figure 5a. The excitation at 600 nm is corresponding to the HOMO-LUMO transition in molecules of Pc, attributed to the $\pi - \pi^*$ transitions in the Pc ring. Intense fluorescence bands at 657 nm and 655 nm for TPP and Pc/TPP, respectively were obtained. Also, it appears an almost imperceptible band at 656 nm for phtalocyanine. A second fluorescence band appears at 694 nm for Pc as also for Pc/TPP; *meso*-tetraphenylporhine shows the fluorescence emission at 710 nm. Under irradiation with light at λ = 320 nm, corresponding to the excitation in the Soret region (not shown here), no fluorescence response appear in the investigated spectral range.

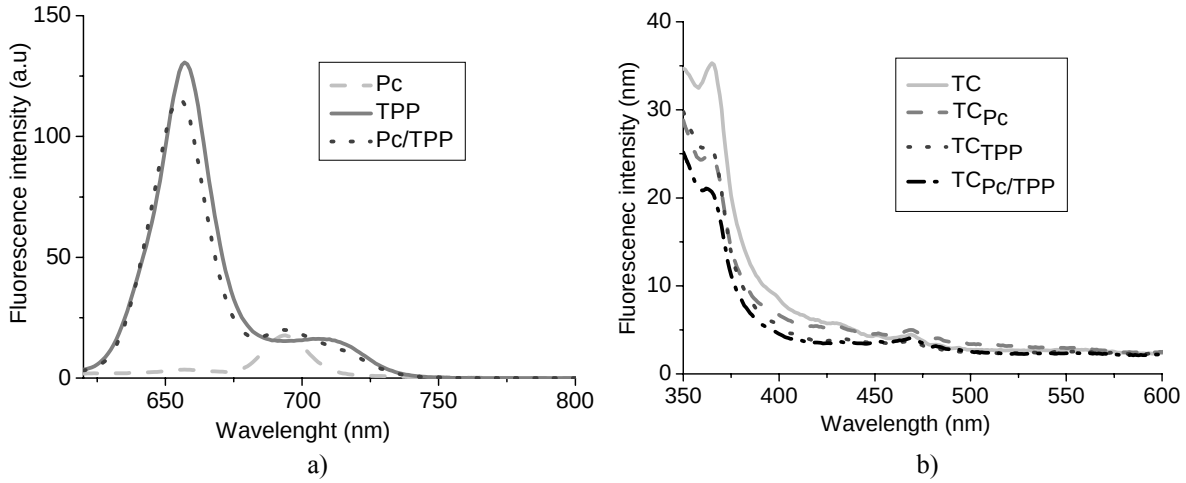

Fig. 5 Fluorescence spectra of: a) PC, TPP and Pc/TPP in dicholorometane and b) TC, TC_{Pc}, TC_{TPP} and $TC_{Pc/TPP}$ samples.

Fig. 5b shows the effect of Pc and TPP on the emission spectra of TiO_2/CdS nanocomposites. No significant changes in fluorescence spectra of TiO_2/CdS-based samples as a result of dyes molecules adsorbed on surface of semiconductor composites were observed.

3.5. FT/IR studies

FT/IR spectra of phthalocyanine and meso-tetraphenylporphine (KBr pellets) together with their vibrational band assignment [42-44] are shown in Figure 6a. In the IR spectra of TiO_2/CdS nanocomposites (sensitized and non-sensitized) several common elements appear: the infrared absorption spectra of phtalocyanine and *meso*-tetraphenylporphine (Figure 6b). The IR spectra of all TiO_2/CdS nanocomposites are characterized by a the broad band of O–H stretching vibration at 3441 cm^{-1} and a weak band at 1629 cm^{-1} due to the deformation vibration (H–O–H) of the physisorbed water molecules [45-48]. The intense broad band located at 520-650 cm^{-1} represents the fundamental vibrations of TiO_2 described by stretching vibrations of Ti–O bonds [45, 48]. The 1122 cm^{-1} band can be attributed to δ(Ti–O–H) deformation vibration [45] of different Ti–OH surface groups. In the 1750-900 cm^{-1} spectral range (Figure 6b, inset spectrum), a number of bands appear that are found in the infrared adsorption of Pc and TPP, which demonstrates their adsorption on the surface of nanocomposites. There are dye frequency shifts in the sensitized composite FTIR spectra as compared to the dye spectra. These frequency shifts can be probably assigned to the physical interactions during the dye adsorption onto the composite surface. The $TC_{Pc/TPP}$ spectrum presents the absorption bands of bond vibrations for both dyes, Pc and TPP, with small shifts in IR spectrum.

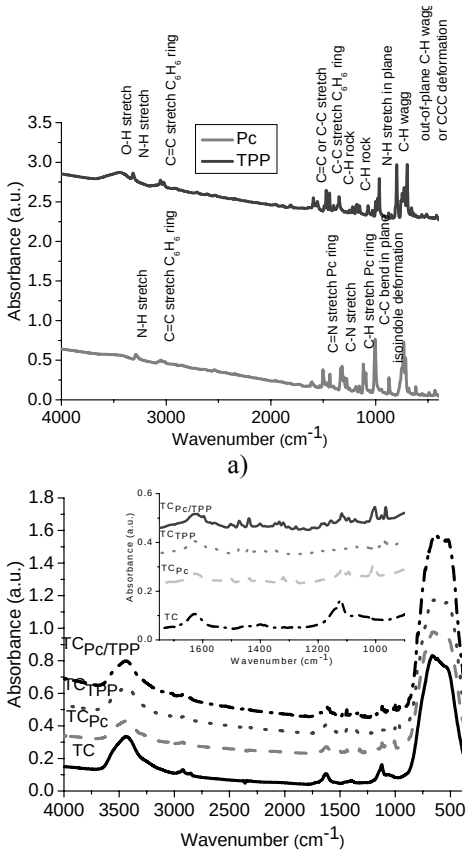

Fig. 6 IR spectra of Pc and TPP powders; inset: IR spectra of TiO_2/CdS samples in restricted area.

3.6. FT/IR microscopy details

The surface morphology of the samples obtained by FT/IR microscopy in transmission mode (square dimensions of 40x40 μm^2) is very different. The Figure 7a shows that the single composite presents a relatively homogeneous distribution of particles. The Figure 7b shows the appearance of crystalline Pc adsorbed on composite surface, filiform shape with dimensions of ~10x5 μm, while TiO_2/CdS nanocomposite sensitized with TPP reveals larger crystals in the branched shape at surface due to the presence of porphyrin-based compound (Figure 7c). The FT/IR microscopy image of surface $TC_{Pc/TPP}$ sample gives morphology information that combines the contributions of both Pc and TPP (Figure 7d).

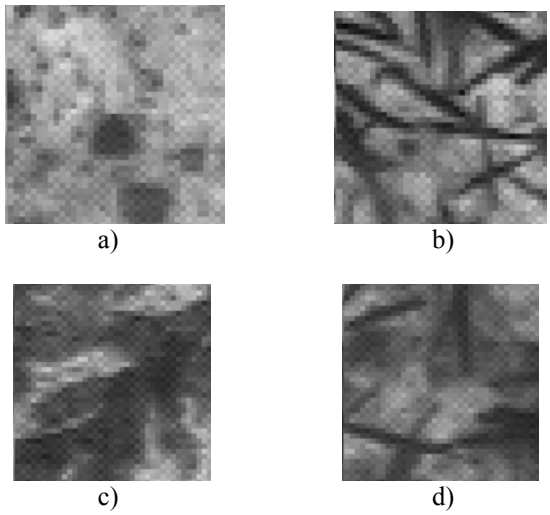

Fig. 7 FT/IR microscopy images of: a) TC, b) TC_{Pc}, c) TC_{TPP} and d) $TC_{Pc/TPP}$.

3.7. Nitrogen adsorbtion-desorbtion isotherms

The specific surface area, pore volume and pore radius of the TiO_2, CdS and TiO_2/CdS nanocomposite were determinate from N_2 adsorption–desorption isotherms (at -196°C), using the BET model for surface area determination and Dollimor-Heal method for volume and radius of pores. The N_2 adsorption–desorption isotherms of TiO_2 powder are of type II with H3 hysteresis-loop (figure 8a), which indicates aggregates of plate-like particles giving rise to slit-shaped pores [49]. The N_2 adsorption–desorption isotherms of CdS powder (Figure 8b) are similar to that of TiO_2 (Fig. 8a) and for the nanocomposite an intermediary hysteresis between H3 and H4 with narrower pores (Figure 8c) is obtained.

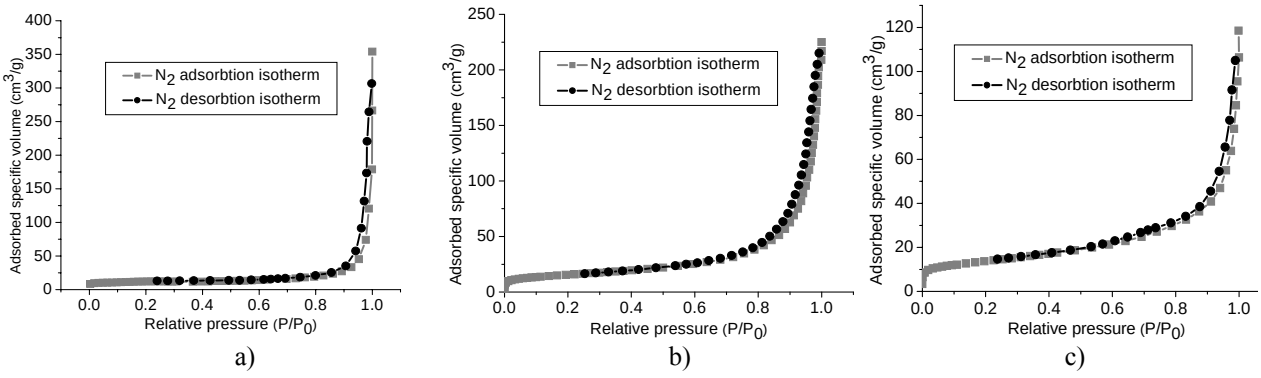

Fig. 8 Nitrogen adsorption–desorption isotherms of: a) TiO_2, b) CdS and c) TiO_2/CdS samples.

The pore size distribution is wide in a range of 25-250 Å for TiO_2 and 75-225 Å for CdS (Figs. 9a and 9b). For TiO_2/CdS nanocomposite (Figure 9c) two types of pores were distinguished: one with the pore radius, R < 50 Å, and the other one with a relatively large distribution between 100 and 225 Å with a maximum at 192 Å. So, the porosity properties of CdS are preserved in the nanocomposite material and also the TiO_2 contribution with smaller radius pores appear. The fraction of the small pore radius appeared in nanocomposite being probably due to the lyophilization process.

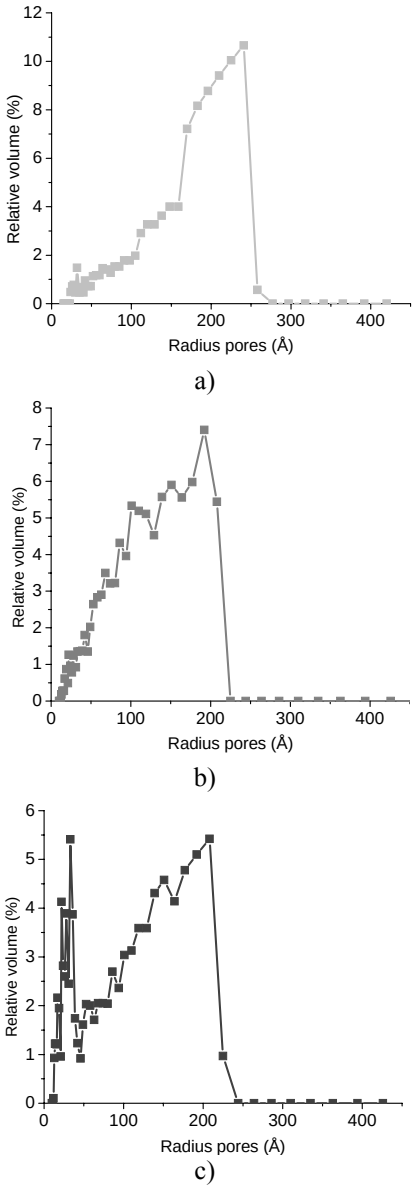

Fig. 9 Pore distributions of: a) TiO_2, b) CdS and c) TiO_2/CdS samples.

Table 2 shows several physical-chemical properties of the TiO_2, CdS and TiO_2/CdS nanocomposite. It is observed that the surface area and the specific pore volume of composite are between those of TiO_2 and CdS.

Table 2. Summary of the physical-chemical properties of the TiO_2, CdS and TiO_2/CdS samples.

Sample's name	S_{BET} (m^2/g)	Specific pore volume (cm^3/g)	Radius pore size (Å)
TiO_2	42.3	0.05	20-250
CdS	55.4	0.13	75-225
TC (TiO_2/CdS)	48.7	0.07	100-225

4. Conclusions

In order to improve the photocatalytic activity of titanium dioxide it was associated with a semiconductor with absorption in visible region of the solar spectrum, namely CdS. The effects of phtalocyanine (Pc) and *meso*-tetraphenylporphine (TPP), as sensitizer dyes on TiO_2/CdS nanocomposites were also investigated in order to increase the electrocatalytic performance of nanocomposite. The TiO_2/CdS nanocomposites could improve its photocatalytic efficiency by formation of highly dispersed composite of TiO_2 and CdS using nanosized materials. The quality of these nanocomposite materials could be also increased by an efficient charge separation, a recombination probability of the electron–hole pairs diminished and an enhancement of photostability. Also, sensitizing the nanocomposites with phtalocyanine and *meso*-tetraphenylporphine causes a photoactivity improvement by the capability of the described dyes to have an intense photon absorption in the visible light domain and the ability of sensitizers to inject the photogenerated electrons from the excited dye molecule into the conduction band of the semiconductor, under visible light action.

Acknowledgements

This work was supported by the Romanian Ministry of Education and Research through program, National Core Project PN 09-44N 02-06. We thank to Degussa AG, Germany for the continuous support of the research team.

References

[1] G. J. Yang, C. J. Li, F. Han, X. C. Huang, J. Vac. Sci. Technol. B **22**, 2364 (2004).
[2] A. K. Jha, K. Prasad, A. R. Kulkarni, Colloids Surfaces B **71**, 226 (2009).
[3] A. Mahyar, M. A. Behnajadi, N. Modirshahla, Indian J. Chem. **49**, 1593 (2010).
[4] M. Bellardita, M. Addamo, A. Di Paola, G. Marcì, L. Palmisano, L. Cassarb, M. Borsa, J. Hazard. Mater. **174**, 707 (2010).
[5] O. Carp, C. L. Huisman, A. Reller, Prog. Solid State. Ch. **32**, 33 (2004).
[6] J. Jun, M. Dhayal, J. H. Shin, J. C. Kim, N. Getoff, Radiat. Phys. Chem. **75**, 583 (2006).

[7] R.S. Mane**,** M. Y. Yoon**,** H. Chung, S. H. Han, Sol. Energy **81**, 290 (2007).
[8] E. G. Seebauer, M. C. Kratzer, Engineering and Materials Processes, Springer-Verlag London Limited (2009).
[9] M. Ştefan, E. – J. Popovici, L. Mureşan, R. Grecu, E. Indrea, J Adv. Mater., 10, 9, 2228-2233 (2008)
[10] F. M. Hossain, L. Sheppard, J. Nowotny, G. E. Murch, J. Phys. Chem. Solids **69**, 1820 (2008).
[11] X. Li, Y. Cheng, L. Liu, J. Mu, Colloids and Surfaces A: Physicochem. Eng. Aspects **353**, 226 (2010).
[12] Q. Xiao, J. Zhang, C. Xiao, Z. Si, X. Tan, Sol. Energy **82**, 706 (2008).
[13] W. Zhao, Z. Bai, A. Ren, B. Guo, C. Wu, Appl. Surf. Sci. **256**, 3493 (2010).
[14] S. Yang, W. Tang, Y. Ishikawa, Q. Feng, Mater. Res. Bull. **46**, 531 (2011).
[15] F. Han, V. Subba, R. Kambala, M. Srinivasan, D. Rajarathnam, R. Naidu, Appl. Catal. A:General **359**, 25 (2009).
[16] C. F. Lin, C. H. Wu, Z. N. Onn, J.Hazard. Mater. **154**, 1033 (2008).
[17] K. Prabakar, H. Seo, M. Son, H. Kim, Mater. Chem. Phys. **117**, 26 (2009).
[18] K. Ravichandran, P. Philominathan, Sol. Energy **82**, 1062 (2008).
[19] J. C. Tristão, F. Magalhães, P. Corio, M. Terezinha C. Sansiviero, J. Photoch. Photobio. A **181**, 152 (2006).
[20] S. Bai, H. Li, Y. Guan, S. Jiang, Appl. Surf. Sci. **257**, 6406 (2011).
[21] H. Jia, H. Xu, Y. Hu, Y. Tang, L. Zhang, Electrochem. Commun. **9**, 354 (2007).
[22] S. P. Mondal, A. Dhar, S. K. Ray, Mat. Sci. Semicon. Proc. **10**, 185 (2007).
[23] J. S. Jang, S. M. Ji, S. W. Bae, H. C. Son, J. S. Lee, J. Photoch. Photobio. A **188**, 112 (2007).
[24] X. Qian, D. Qin, Q. Song, Y. Bai, T. Li, X. Tang, E. Wang, S. Dong, Thin Solid Films **385**, 152 (2001).
[25] Y. J. Chi, H. G. Fu, L. H. Qi, K. Y. Shi, H. B. Zhang, H. T. Yu, J. Photoch. Photobio. A **195**, 357 (2008).
[26] A. Huijser, T. J. Savenije, L. D. A. Siebbeles, Thin Solid Films **511–512**, 208 (2006).
[27] A. Kathiravan, R. Renganathan, J.Colloid Interf. Sci. **331**, 401 (2009).
[28] C. Wang, G. M. Yang, J. Li, G. Mele, R. S1ota, M. A. Broda, M. Y. Duan, G. Vasapollo, X. Zhang, F. X. Zhang, Dyes Pigments **80**, 321 (2009).
[29] H. Karaca, S. Sezer, C. Tanyeli, Dyes Pigments **90**, 100 (2011).
[30] G. Zanotti, N. Angelini, S. Notarantonio, A. M. Paoletti, G. Pennesi, G. Rossi, A. Lembo, D.Colonna, A. Di Carlo, A. Reale, T. M. Brown, G. Calogero, Int. J. Photoenergy 1 (2011), doi:10.1155/2010/136807
[31] E. Palomares, M. V. Martínez-Díaz, S. A. Haque, T. Torres, J. R. Durrant, Chem. Commun. 2112 (2004).
[32] Md. K. Nazeeruddin, R. Humphry-Baker, M. Grätzel, D. Wöhrle, G. Schnurpfeil,G. Schneider, A. Hirth, N. Trombach, J. Porphyrins Phthalocyanines **3**, 230 (1999).
[33] V. N. Nemykin, E. A. Lukyanets, Arkivoci 136 (2010).
[34] G. Palmisano, M. C. Gutiérrez, M. L. Ferrer, M. D. Gil-Luna, V. Augugliaro, S. Yurdakal, M.Pagliaro, J. Phys. Chem. C **112**, 2667 (2008).
[35] J. M. Huijser, 2008, ISBN 978-90-6464-229-6.
[36] J. Janczak, Pol. J. Chem. **74**, 157 (2000)
[37] S. J. Silvers, A. Tulinsky, J. Am. Chem. **89**, 3331 (1967)
[38] D. Vlascici, A. Chiriac, E. Făgădar-Cosma, O. Spiridon-Bizerea, R. Tudose, Annals of West University of Timisoara, Series Chemistry **13**, 9 (2004).
[39] Y. H. Zhang, C. Ma, L. Guo, Q. S. Li, Chinese Chem. Lett. **11**, 555 (2000).
[40] G. L. Pakhomov, D. M. Gaponova, A. Yu. Luk'yanov, E. S. Leonov, Phys. Solid State+ **47**, 170 (2005).
[41] Ot. E. Sielcken, M. M. van Tilborg, M. F. M. Roks, R. Hendriks, W. Drenth, R. J. M. Nolte, J. Am. Chem. Soc. **109**, 4261 (1987).
[42] X. X. Zhang, M. Bao, N. Pan, Y. X. Zhang, J. Z. Jiang, Chinese J. Chem. **22**, 325 (2004).
[43] A. V. Udal'tsov, G. Kaupp, A. I. Taskaev, Colloid J. **66**, 489 (2004).
[44] L. C. Xu, Z. Y. Li, W. Tan, T. J. He, F. C. Liu, D. M. Chen, Spectrochim. Acta A **62**, 850 (2005).
[45] T. Bezrodna, G. Puchkovska, V. Shymanovska, J. Baran, H. Ratajczak, J.Mol. Struct. **700**, 175 (2004).
[46] N. Venkatachalam, M. Palanichamy, V. Murugesan, Mater. Chem. Phys. **104**, 454 (2007).
[47] Wug-Dong Park, Trans. Electr. Electron. Mater. **11**, 170 (2010).
[48] M. Hamadanian, A. Reisi-Vanani, A. Majedi, Appl. Surf. Sci. **256**, 1837 (2010).
[49] K. S. W. Sing, D. H. Everett, R. A. W. Haul, L. Moscou, R. A. Pierotti, J. Rouquerol, T.Siemieniewska, Pure & Appl. Chem. **57**, 603 (1985).

*Corresponding author: marcela.rosu@itim.cj.ro